Article

Not peer-reviewed version

Selective Functionalization of Carbonyl Closo-Decaborate [2-$B_{10}H_9CO]^-$ with Building Block Properties via Grignard Reagents

Nadine Mahfouz *, Fatima Abi Ghaida *, Wael Kotob , Ahmad Mehdi *, Daoud Naoufal *

Posted Date: 10 July 2023

doi: 10.20944/preprints202307.0550.v1

Keywords: Hydroborate; closo-decaborate; Grignard reagents RMgX; building blocks [2- B10H9COR]2-

Article

Selective Functionalization of Carbonyl Closo-Decaborate $[2\text{-}B_{10}H_9CO]^-$ with Building Block Properties via Grignard Reagents

Nadine Mahfouz [1,2], Fatima Abi-Ghaida [1,*], Wael Kotob [1], Ahmad Mehdi [2,*] and Daoud Naoufal [1,*]

[1] Inorganic and Organometallic Coordination Chemistry Laboratory LCIO, Lebanese University, Faculty of Sciences, Lebanon, dnaoufal@ul.edu.lb, fghaida@ul.edu.lb

[2] Institut Charles Gerhardt ICGM, Université de Montpellier, CNRS, ENSCM, Montpellier, 34090, France, ahmad.mehdi@umontpellier.fr

* Correspondence: fghaida@ul.edu.lb, ahmad.mehdi@umontpellier.fr, dnaoufal@ul.edu.lb.

Abstract: A green, fast and selective approach for the synthesis of mono-substituted closo-decaborate derivatives $[2\text{-}B_{10}H_9COR]^{n-}$ has been established via a nucleophilic addition reaction between the carbonyl derivative of closo-decaborate $[2\text{-}B_{10}H_9CO]^-$ and the corresponding Grignard reagent RMgX, where R is the ethyl, iso-propyl, pentyl, allyl, vinyl, and propynyl groups. This approach is accomplished under mild conditions with 70–80% yields. The significance of these derivative is their ability to constitute building blocks for polymeric integration via the allyl, vinyl and propynyl substituents. All products were characterized by ^{11}B, ^{1}H, and ^{13}C NMR, elemental analysis and mass spectrometry.

Keywords: Hydroborate; *closo*-decaborate; Grignard reagents RMgX; building blocks $[2\text{-}B_{10}H_9COR]^{2-}$

1. Introduction

The *closo*-borate anions $[B_nH_n]^{2-}$ (n = 6 -12), particularly the *closo*-decaborate $[B_{10}H_{10}]^{2-}$, represent one of the most confounding and appealing compounds in polyhedral architecture.[1–3] Their physiochemical properties as thermodynamic stability,[4] electrochemical properties,[5,6] three-dimensional aromaticity,[3] modulated biological compatibility,[7,8] as well as their tunable hydrophobicity has encouraged their integration in a litany of applications ranging from metal complexation,[9] medicine[7] and catalysis[10] to material sciences,[11–13] solid state batteries,[14–16] and hydrogen storage.[17,18] Functionalized or derivatized protagonists of the polyhedral boron clusters are often regarded as versatile and circumventive building blocks; indeed, the pharmacological aptitudes of these three-dimensional inorganic cages are often comparable to that of the three-dimensional coveted diamondoid cages of adamantine, but with far more desired electronic properties that infer their derivatives with stabilizing properties.[19] For example, reactive nitrilium derivatives of the *closo*-borate anions often retain their stability and structural integrity under mild aerobic, acidic, or basic conditions which render them suitable for in-situ physiological applications.[20] Pharmacologically oriented research on boron clusters currently focuses on their coalescence within self-sufficient systems of diagnostics and treatment, their unique features as selective receptor agonists are preferable to classical organic scaffolds and are frequently exploited in further elucidation of structure activity relationship (SAR) profiles.[21] One of the long-standing medicinal applications of boron clusters is boron neutron capture therapy (BNCT), a preferential and theoretically infallible targeted therapy regime that exploits boron-10 isotopes' susceptibility to thermal neutrons.[22] The BNCT protocol or more precisely the boron-10 enriched functionalized clusters suffer from non-preferential and inadequate accumulation within the tumor cells due to the lack of selective carriers; hence, a universally and medically acquiesced BNCT protocol demands

Preprints (www.preprints.org) | NOT PEER-REVIEWED | Posted: 10 July 2023 doi:10.20944/preprints202307.0550.v1

establishing a synergistic unified system comprising boron-10 sources and targeting carriers. Recently, Yorov *et al.* immobilized an alkoxysilane derivative bearing a 10-vertex closo-decaborate nanocluster in a silica (SiO_2) aerogel matrix. The silica nanomaterial loaded with 1.2 mol % closo-decaborate possessed high specific surface area (740 m^2/g), low apparent density (80 mg/cm^3) and exhibited low toxicity towards normal cells and considerable cytotoxicity towards malignant glioblastoma cells.[23] The strategy was first introduced in 2014 where the authors reported the first-in-class borate-alkoxysilane derivatives via the functionalization of the carbonyl- and diazo-derivatives of closo-decaborate and validated the integrity/activity of the precursors to integrate into the matrix, pores, and surfaces of silica-based nanomaterial (biologically compatible mesoporous silica and silica nanoparticles) as proof of concept.[24,25] Another synergistic carrier was introduced by Stepanova *et al.* to combine boron delivery to the tumor cells of osteosarcoma and the repair of postoperative bone defects, the authors reported boron-containing scaffolds comprising novel biodegradable polymer composites as films and 3D-printed matrices based on aliphatic polyesters containing closo-borates clusters for BNCT.[26]

The impediment in integrating inorganic boron-based polyhedral archetypes such as the anionic closo-decaborate $[B_{10}H_{10}]^{2-}$ and the closo-dodecaborate $[B_{12}H_{12}]^{2-}$ into industrial or pharmacological venues lies in the introduction of functional groups into theses clusters.[27–31] Indeed, the ability to engineer functional boron-enriched materials via derivatization of the clusters, or what is rather known as the activation of one or more exo-polyhedral B-H bonds, is often constrained for compounds with a purely boron skeleton as opposed to their neutral carbon-enclosing analogs as the icosahedral dicarba-closo-dodecaborane $[C_2B_{10}H_{12}]$.[32] The polyhedral carboranes rather possess an intrinsic advantage that fundamentally bridges the chemistry of boron clusters with the vast and established chemistry of carbon-based scaffolds, the B-C-H bonds (Figure 1); thus, these compounds have become quite favored in research and industry and have been profoundly investigated in establishing antitumor, antimicrobial and antiviral formulations [33] via their integration into the structure of existing conventional drugs or prodrugs to alter SAR profiles.[34,35] The functionalization pathways of carboranes are quite vast and established, the most recent approach reported direct B–H functionalization of icosahedral carboranes at the most electron-rich boron vertex; that is, the boron vertex with the lowest B–H bond dissociation energy, where a nitrogen-centered radical-mediated hydrogen atom transfer instigated the homolysis of the B–H bond.[36] Conventionally recognized pathways include Metal-catalyzed cross-coupling reactions for assembling larger molecules via covalently bonded molecular fragments,[37] the Sonogashira,[38] Heck,[39] and Suzuki cross-coupling reactions,[40] the Kumada-Corriu cross-coupling reactions between B-iodo-carboranes and Grignard reagents in the presence of palladium-based catalysts.[41] A nucleophilic substitution Grignard reaction pathway was also established for B−H bond activation of ortho-carboranes in the absence of any transition metal catalysts; however, the reaction necessitates the presence of two electron-withdrawing aryl groups on the cage carbon atoms.[42]

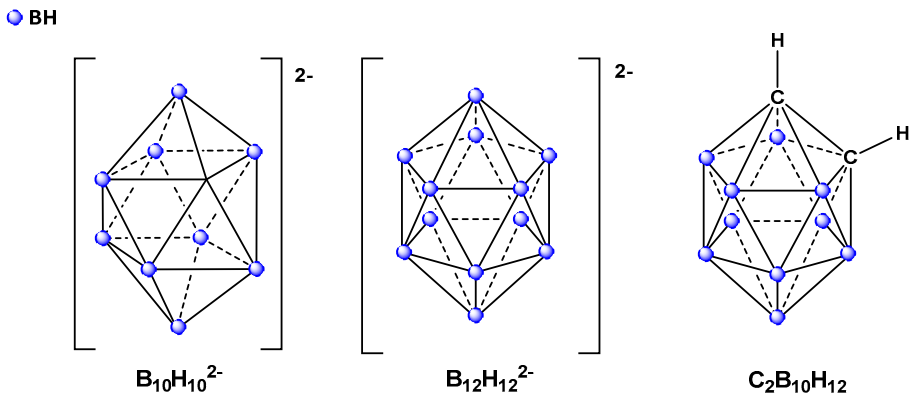

Figure 1. Schematic representation of the closo-decaborate anion, closo-dodecaborate anion, and the neutral icosahedral carborane.

Preprints (www.preprints.org) | NOT PEER-REVIEWED | Posted: 10 July 2023 doi:10.20944/preprints202307.0550.v1

The impedance in the functionalization of the *closo*-decaborate anion is primarily dictated by the electronic environment of the cage; this can be quite challenging due to the presence of 10 inert B–H bonds in a rather stable and comparable chemical environment, B-H bond substitution can proceed via electrophilic or nucleophilic mechanisms in either apical (boron atoms with a coordination number of 4) or equatorial (boron atoms with a coordination number of 5) positions to yield mono-, di- and poly-substituted derivatives [27,30,31,43]. A recent soft approach utilized an auto-catalyzed reaction pathway to functionalize $(NH_4)_2[B_{10}H_{10}]$ by exploiting the in-situ NH_4^+ counter cation during the nucleophilic addition of nitriles to the borate cluster via Electrophilic-Induced Nucleophilic Substitution mechanism.[44,45]

One of the foremost derivatives of the closo-decaborate anion is the carbonyl protagonist $[1\text{-}B_{10}H_9CO]^-$ [46] which has been repeatedly employed as a precursor for further functionalization of the decaborate cage. The carbonyl-mediated reaction pathway has been presented as an alternative to direct alkylation of the closo-decaborate which predominantly necessitates manipulations with nido-decaborane $B_{10}H_{14}$ under unfavorable conditions and yields poly-substituted derivatives. Recently, a direct alkylation strategy of the B–H bond in closo-decaborate was reported by Kaszynski *et al.* following a Pd-catalyzed cross-coupling reaction approach via iodo precursors which has been extensively applied for substitutions of 12-vertex carboranes and dodecaborate anion.[47] Establishing a direct B–C bond in $[B_{10}H_{10}]^{2-}$ has mainly been hindered by the lack of access to suitable precursors such as the iodo-derivatives of decaborate anion which exhibits a practically diminutive reactivity toward iodination (Figure 2). The authors attempted to synthesize the $[closo\text{-}1,10\text{-}B_{10}H_8\text{-}I_2]^{2-}$ anion from the bis-iodonium zwitterion $[closo\text{-}1,10\text{-}B_{10}H_8\text{-}(IPh)_2]$ through Grignard reagents (proven successful for carboranes as the $[closo\text{-}CB_{11}H_{11}I]^-$) but isolation proved ineffective due to the formation of insoluble magnesium salts and instead diverted to organolithium reagents.

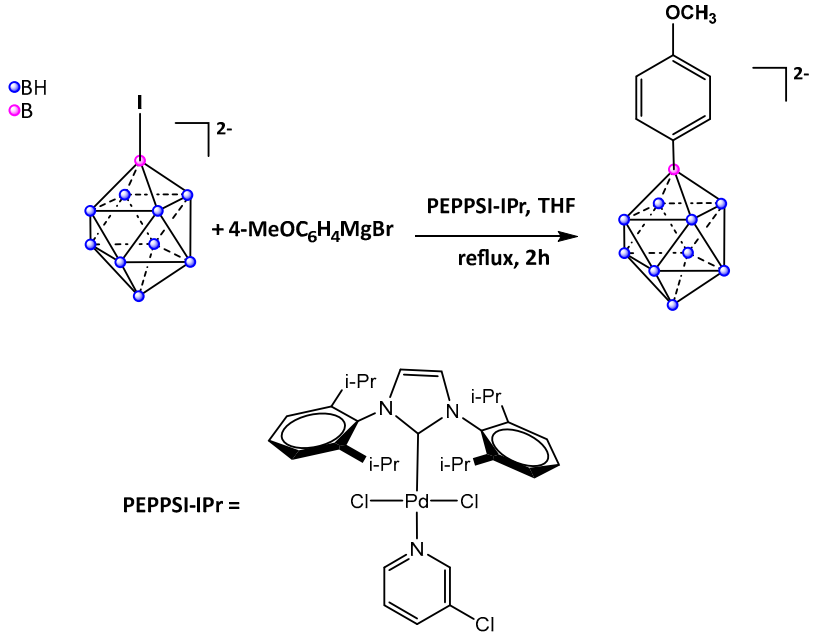

Figure 2. Synthesis of compound with B-C bond from iodo-closodecaborate derivative.

Though the carbonyl derivative is prone to facile and rapid hydrolysis leading to the carboxylic derivative $[1\text{-}B_{10}H_9COOH]^{2-}$ and its manipulation normally requires extremely anhydrous and inert conditions, it is still the preferable precursor of choice due to the versatility supplied by the carbonyl group. Moreover, new reaction pathways for the selective functionalization of this derivative are currently under investigation as conventional approaches suffer from nonselective side reactions as it is easily susceptible to a wide range of functional groups.[48,49] Thus, the main notion of the present work is to establish a selective synthesis route starting from the carbonyl derivative of closo-decaborate to compounds decorated with alkyl chains such as ethyl, propyl, and pentyl chains as well as building block "polymerizable" or "conjugative" constituents such as the allyl, vinyl, and

Preprints (www.preprints.org) | NOT PEER-REVIEWED | Posted: 10 July 2023 doi:10.20944/preprints202307.0550.v1

propynyl derivatives. The necessity of such alkylated and conjugable boron clusters is frequently noted for biological applications as antimicrobial applications [50] and boron neutron capture therapy; indeed, fabricating such derivatives enclosing a hydrophilic charged head (anionic boron cluster) and a hydrophobic tail (alkyl chain) render them as ideal candidates for incorporation into physiological media such as lipophilic bilayers and uni-lamellar liposome penetration; particularly as liposomes have been proven to preferentially localize in tumor cells. Currently, boron-loaded liposomes are under investigation as self-sufficient systems for BNCT cancer treatment.[51]

2. Results

Herein, we report the facile and selective synthesis of versatile *closo*-decaborate derivatives comprising alkyl chains as the propyl and pentyl chains and building blocks as the allyl, vinyl, and propynyl groups. The novel synthesis approach proceeds via a straightforward nucleophilic addition reaction at room temperature between the carbonyl derivative of closo-decaborate (PPh_4) [$B_{10}H_9CO$] and a Grignard reagent RMgX comprising the desired functionality under an inert atmosphere.

First, we prepared the compound carbonyl-closodecaborate (PPh_4)[2-$B_{10}H_9CO$] by the reaction of (PPh_4)$_2$[$B_{10}H_{10}$] with excess of oxalyl chloride $(COCl)_2$ in the solvent dichloromethane and at 0 °C (Figure 3A) following the described method.[46]

Second, six different Grignard reagents were used ranging from simple alkyl as the ethyl, iso-propyl, and pentyl to the allyl, vinyl, and propynyl groups (Figure 3B); three of which encompass building block functionalities for further conjugation or polymerization of the *closo*-decaborate cluster into functional materials.

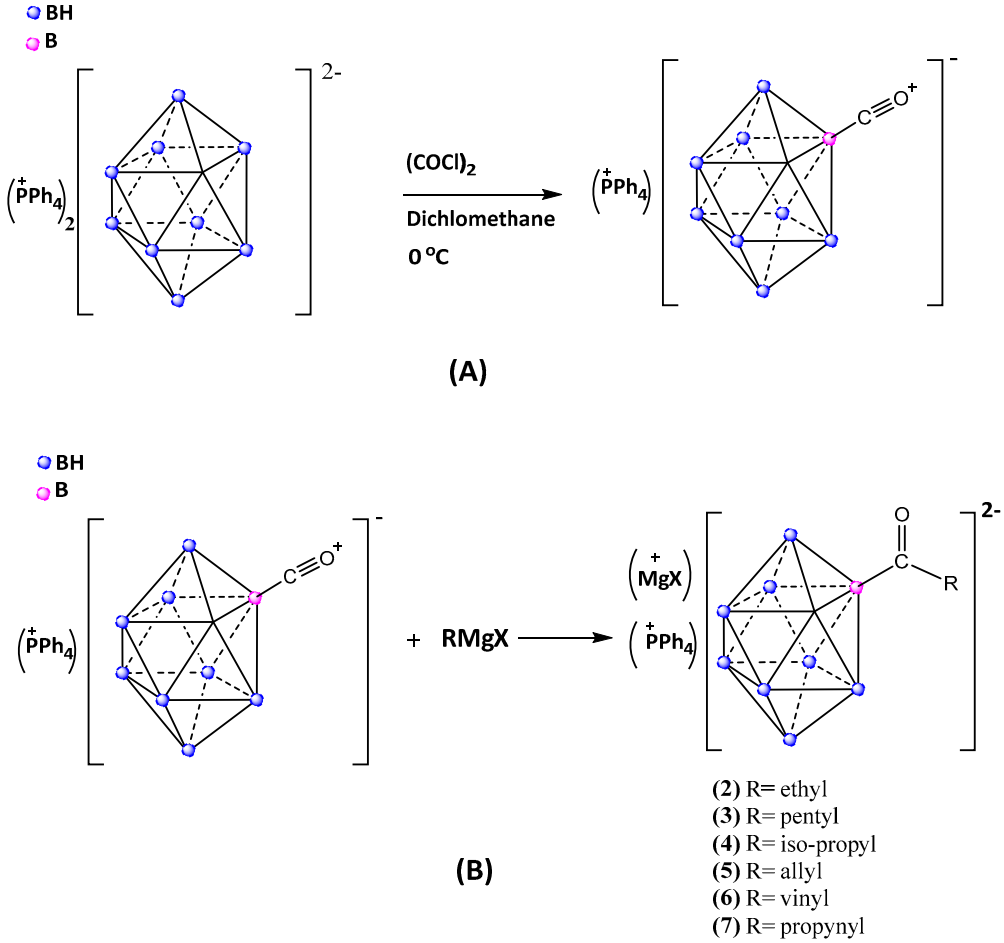

Figure 3. Schematic representation of the synthesis of carbonyl-closodecaborate (A) and the nucleophilic addition of Grignard reagents to the carbonyl derivative of closo-decaborate (B).

Preprints (www.preprints.org) | NOT PEER-REVIEWED | Posted: 10 July 2023 doi:10.20944/preprints202307.0550.v1

The nucleophilic addition of alkyl Grignard reagents as the ethyl, iso-propyl, and pentyl magnesium bromide to the carbonyl derivative yields the corresponding carbonyl-alkyl derivatives $[2\text{-}B_{10}H_9C(O)CH_2CH_3]^{2-}$ (**2**), $[2\text{-}B_{10}H_9C(O)C_3H_7]^{2-}$ (**3**), and $[2\text{-}B_{10}H_9C(O)C_5H_9]^{2-}$ (**4**), isolated by mere precipitation out of the reaction mixture via diethyl ether and filtration. The structural integrity of the *closo*-derivatives was verified through multinuclear NMR where the ^{11}B NMR exhibits the appearance of a singlet at approximately -20 ppm (Figure 4) for the equatorially substituted boron of $[2\text{-}B_{10}H_9C(O)CH_2CH_3]^{2-}$ (**2**) and $[2\text{-}B_{10}H_9C(O)C_5H_9]^{2-}$ (**3**) in place of the singlet corresponding to the carbonyl derivative $[2\text{-}B_{10}H_9CO]^-$ at -44.7 ppm while the isopropyl derivative $[2\text{-}B_{10}H_9C(O)C_3H_7]^{2-}$ (**4**) singlet appears at -19.10 ppm (see Figure S1 in the ESI).

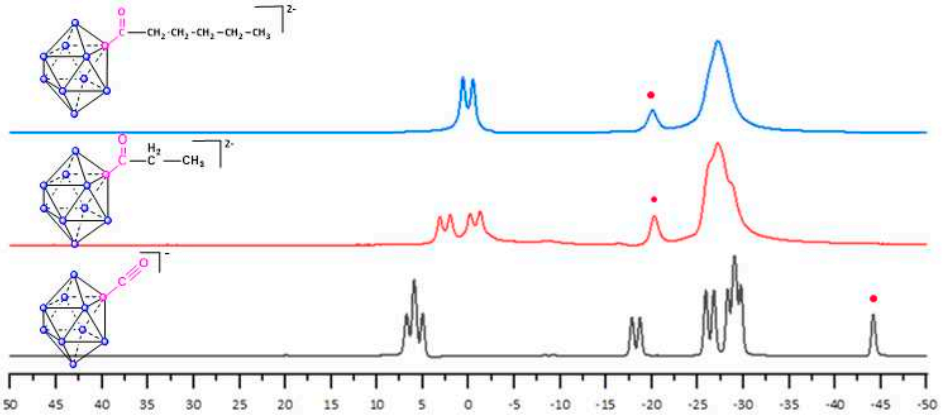

Figure 4. B NMR spectrum of carbonyl-closo-decaborate derivative $[2\text{-}B_{10}H_9CO]^-$ (**1**), $[2\text{-}B_{10}H_9C(O)CH_2CH_3]^{2-}$(**2**), $[2\text{-}B_{10}H_9C(O)C_5H_9]^{2-}$(**3**).

^1H and ^{13}C NMR display the characteristic peaks of the ethyl, isopropyl and pentyl groups. ^1H NMR (Figure 5) of $[2\text{-}B_{10}H_9C(O)CH_2CH_3]^{2-}$ (**2**) exhibits a doublet at 0.65 ppm for – CH_3 and a quadruplet at 2.23 ppm for – CH_2 while the ^{13}C NMR (Figure 6) exhibits a peak at 157.30 ppm for the carbonyl group, a peak for the sp^3 carbon in CH_3 at 1.13 ppm and another peak at 8.65 ppm for –CH_2. Similarly, the ^1H NMR (see Figure S10 in the ESI) of $[2\text{-}B_{10}H_9C(O)C_3H_7]^{2-}$ (**4**) displays a doublet at 0.68 ppm for the CH_3 groups present in the product and a sextuplet at 2.65 ppm for -CH while the ^{13}C NMR (see Figure S11 in the ESI) shows a peak at 19.59 ppm for the sp^3 carbon in CH_3. Finally, for the compound with pentyl group $[2\text{-}B_{10}H_9C_5H_9]^{2-}$ (**3**), the ^1H NMR (see Figure S6 in the ESI) exhibits a triplet at 0.75 ppm for -CH_3, a sextuplet at 1.10 ppm for -CH_2, a quintuplet at 1.25 ppm for -CH_2 and a triplet at 2.15 ppm for -C(O)CH_2. In addition, the ^{13}C NMR (see Figure S7 in the ESI) exhibits a peak at 166.35 ppm for the carbonyl group, a peak at 14.32 ppm for the sp^3 carbon in -CH_3 and another peaks at 22.72 ppm, 24.18 ppm and 32.10 ppm for the -CH_2 in the compound. The counter ion PPh_4^+ was also detected by the appearance of a singlet in the ^{31}P NMR at 22.59 ppm showing the presence of phosphonium ion in the compound (**2**) (see Figure S4 in the ESI).

Preprints (www.preprints.org) | NOT PEER-REVIEWED | Posted: 10 July 2023 doi:10.20944/preprints202307.0550.v1

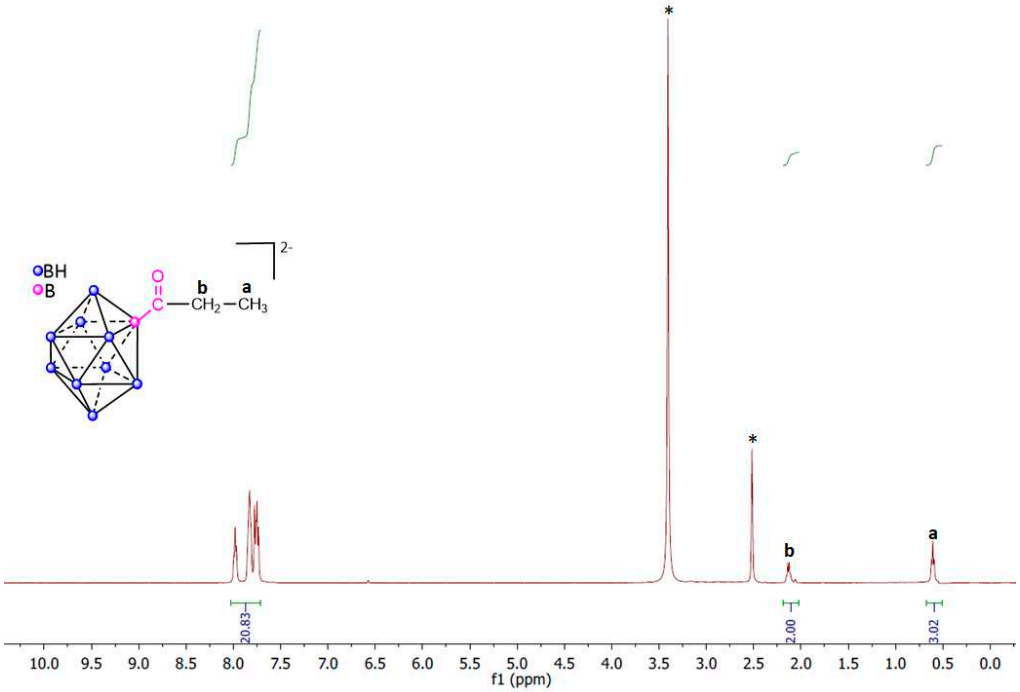

Figure 5. H NMR spectrum of the compound $[2\text{-}B_{10}H_9C(O)CH_2CH_3]^{2-}$ (**2**).

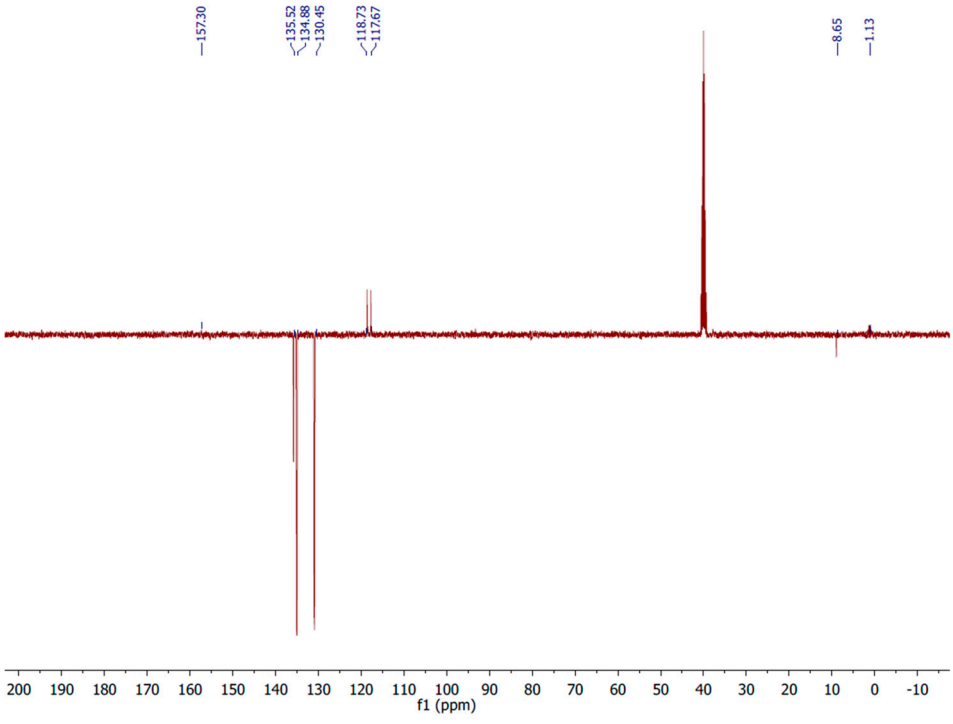

Figure 6. C NMR spectrum of the compound $[2\text{-}B_{10}H_9C(O)CH_2CH_3]^{2-}$ (**2**).

To assert the necessity of the carbonyl group and further elucidate the nucleophilic addition mechanism, several control reactions were performed between the tetraphenylphosphonium salts of the *closo*-decaborate anion $[B_{10}H_{10}]^{2-}$, the undecahydro-*closo*-decaborate anion $[B_{10}H_{11}]^{-}$ and the corresponding Grignard reagents. ^{11}B NMR indicated the absence of any functionalization or degradation of the decaborate cluster for the reaction of the *closo*-decaborate anion $[B_{10}H_{10}]^{2-}$ with RMgBr and suggests only the precipitation of the MgBr salt of the cage. Moreover, the second control

Preprints (www.preprints.org) | NOT PEER-REVIEWED | Posted: 10 July 2023 doi:10.20944/preprints202307.0550.v1

reaction of the undecahydro-*closo*-decaborate anion $[B_{10}H_{11}]^-$ and RMgBr suggests a complexation reaction taking place between $[B_{10}H_{10}]^{2-}$ and the metallic center Mg^{2+} as the ^{11}B NMR displays a shift in the boron atoms peak in apical position from 0 ppm to 3 ppm and another peak shift of equatorial boron atoms from -30 ppm to -26 ppm.

An identical synthesis methodology was used to functionalize the *closo*-decaborate carbonyl derivative with potential building block substituents comprising the allyl, vinyl, and propynyl functionalities. The fairly straightforward synthesis involved the preparation of an etherate solution of $(PPh_4)[B_{10}H_9CO]$ in anhydrous THF under argon and the corresponding Grignard reagent (allyl magnesium bromide, vinyl magnesium bromide, and propynyl magnesium bromide) added dropwise. Isolation of the respective products yielded the phosphonium salts of $[2\text{-}B_{10}H_9C(O)CH_2CH{=}CH_2]^{2-}$ (**5**), $[2\text{-}B_{10}H_9C(O)CH{=}CH_2]^{2-}$(**6**), and $[2\text{-}B_{10}H_9C(O)C{\equiv}CCH_3]^{2-}$ (**7**) derivatives, respectively. ^{11}B NMR data clearly display a shift in the carbonyl singlet from − 44.7 ppm to -20.17, -18.62, and -18.22 ppm for the allyl, vinyl, and propynyl derivatives (see Figure S1 in the ESI). The deshielding effect in the vinyl and propynyl derivatives can be explicitly attributed to the electronic resonance between the double and triple bonds of the vinyl and propynyl groups and the oxygen lone pairs. ^1H NMR and ^{13}C NMR clearly display the characteristic peaks of the corresponding allyl and vinyl groups where the $-CH{=}CH_2$ in $[2\text{-}B_{10}H_9C(O)CH_2CH{=}CH_2]^{2-}$ (**5**) appears at 4.85 and 5.85 ppm in ^1H NMR and 117.65 and 135.29 ppm in ^{13}C NMR (see Figure S14 in the ESI). For the vinyl group in the compound $[2\text{-}B_{10}H_9C(O)CH{=}CH_2]^{2-}$ (**6**), the ^1H NMR and ^{13}C NMR prove his formation by the appearance of peaks at 4.95 ppm, 5.85 ppm and 6.49 ppm in ^1H NMR and 130.91 ppm and 135.95 ppm in ^{13}C NMR (see Figure S17 in the ESI). For the $[2\text{-}B_{10}H_9C(O)C{\equiv}CCH_3]^{2-}$ (**7**) derivative, his formation was confirmed by ^1H NMR (Figure 7): appearance of singlet at 1.75 ppm for the $-CH_3$ and by ^{13}C NMR (Figure 8): appearance of three peaks at 3.91 ppm, 67.50 ppm and 82.50 ppm. In addition, the MS spectra (Figure 9) of this compound prove the formation of the new product such as $[2\text{-}B_{10}H_9C(O)C{\equiv}CCH_3]^{2-}$ (**7**) by appearance of two signals at 184.0 and 524.32.

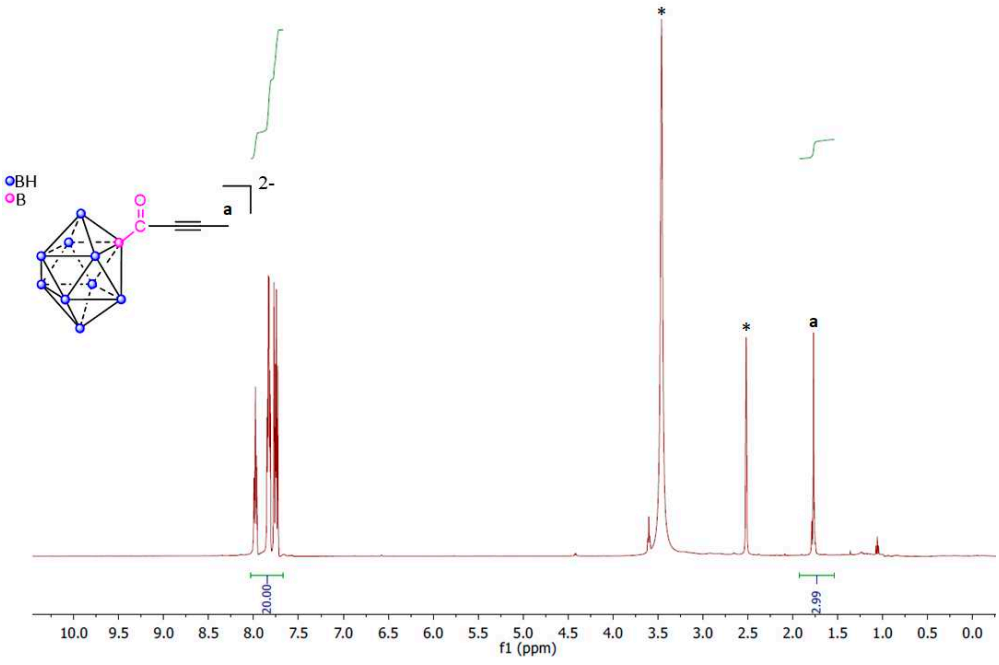

Figure 7. H NMR spectrum of the compound $[2\text{-}B_{10}H_9C(O)C{\equiv}CCH_3]^{2-}$ (**7**).

Preprints (www.preprints.org) | NOT PEER-REVIEWED | Posted: 10 July 2023 doi:10.20944/preprints202307.0550.v1

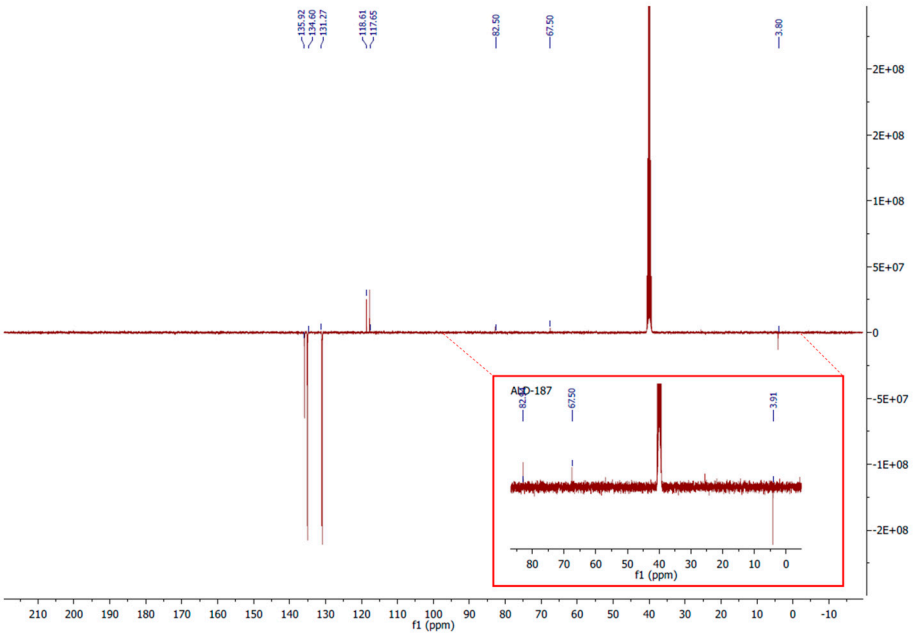

Figure 8. C NMR spectrum of the compound $[2\text{-}B_{10}H_9C(O)C{\equiv}CCH_3]^{2-}$ (**7**), the inset is the zoomed part that shows the three types of carbons in the compound (**7**).

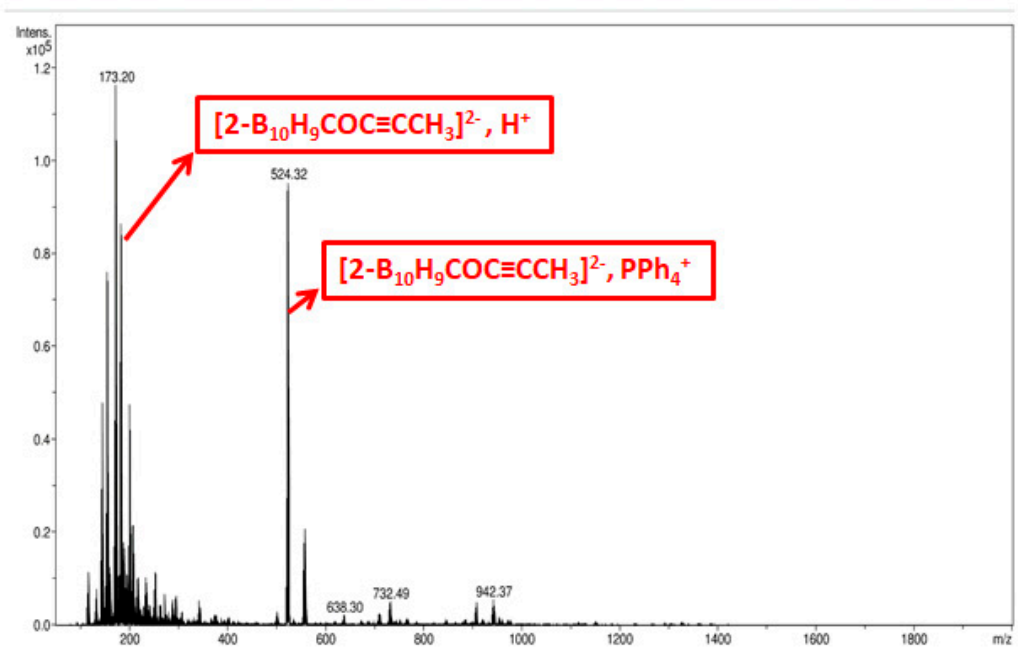

Figure 9. MS spectrum of the compound $[2\text{-}B_{10}H_9C(O)C{\equiv}CCH_3]^{2-}$(**7**).

3. Materials and Methods

All reactions were performed under an inert atmosphere (Argon) using vacuum tube and Schlenk techniques. All solvents used in the syntheses were dried and distilled accordingly. $(Et_3NH)_2[B_{10}H_{10}]$ was purchased from Boron Specialties (United States) and the salt $(PPh_4)_2B_{10}H_{10}$ was precipitated from an aqueous solution of $(Et_3NH)_2B_{10}H_{10}$ and recrystallized from an acetonitrile–Et_2O mixture. Ethyl magnesium Bromide, pentyl magnesium bromide, iso-propyl magnesium chloride, allyl magnesium chloride, vinyl magnesium bromide and 1-propynyl magnesium bromide were purchased from Sigma-Aldrich and used as received. Oxalyl chloride was obtained as 2.0 M solution

 doi:10.20944/preprints202307.0550.v1

in CH_2Cl_2 from Aldrich. Solution ^{1}H-NMR spectra was recorded using an AMX 400 Bruker spectrometer operating respectively at 400 MHz. For the analysis of our boron-based products, the ^{11}B sequence used has the following characteristics: ^{11}B spectra were recorded at 298 K on a Bruker Advance III 500 Mz NMR spectrometer equipped with a BBO helium cryoprobe. The ^{11}B zgbs pulse sequence is used with a spectral width of 64102 Hz and 256 scans with a relaxation time of 0.5 s. Chemical shifts were externally calibrated to TMS for ^{1}H and $EtO_2{\cdot}BF_3$ for ^{11}B nuclei. Deuterated DMSO and acetonitrile were used as solvents. Mass spectrometry measurements were performed by negative electrospray ionization method (ESI/MS).

Synthesis of carbonyl-closo-decaborate (PPh_4) [$B_{10}H_9CO$] (1)

(PPh_4) [2-$B_{10}H_9CO$] (1) was prepared according to the literature with 74% yield after crystallization from CH_2Cl_2–Et_2O. **^{11}B (^{1}H) NMR** (δ ppm, 128 MHz, CD_3CN): 5.3 (d, 2B), -18.7 (d, 1B), -26.8 (d, 2B), -28.1 (d, 2B), -29.8 (d, 2B), -44.7 (s, 1B).

Synthesis of closo-decaborate derivatives (PPh_4)[$B_{10}H_9COR$]

A solution containing 200 mg of (PPh_4) [2-$B_{10}H_9CO$] and 10 mL of anhydrous THF was placed under argon at room temperature where one equivalent of the corresponding Grignard reagent RMgX was added dropwise. The reaction progress was monitored periodically by TLC (DEAE-Cellulose) where the complete disappearance of the carbonyl derivative was noted after 10 minutes of stirring. The reaction volume was reduced by 2/3 and placed at -20 °C; the targeted products precipitated out of the mixture and were isolated as pale-yellow solids.

(PPh_4)(MgBr)[2-$B_{10}H_9C(O)CH_2CH_3$] (**2**) **^{11}B (^{1}H) NMR** (δ ppm, 128 MHz, CD_3CN): 2.59 (d, 1 B), -0.77 (d, 1 B), -20.21 (s, 1 B), between -25.39 and -29.41 (m, broad, 7 B). **^{1}H NMR** (δ ppm, DMSO-d6): 0.65 (3 H, d, CH_3), 2.23 (2 H, quadruplet, CH_2), 7.5-7.8 (20 H, m, H of PPh_4^+). **^{13}C NMR** (δ ppm, DMSO-d6): 157.30, 135.52, 134.88, 130.45, 118.73, 117.67, 8.65, 1.13. **^{31}P NMR** (DMSO-d6): 22.58. **Mass spectrometry (ESI/MS):** m/z = 172.19 **Elemental analysis:** % theoretical C: 52.512; H: 5.510. Found C: 48.266; H: 6.711. H/C ratio: 0.12. **Yield:** 85%.

(PPh_4)(MgBr)[2-$B_{10}H_9C(O)C_5H_9$] (**3**) **^{11}B (^{1}H) NMR** (δ ppm, 128 MHz, CD_3CN): 0.23 (d, 2 B), -19.98 (s, 1 B), between -24.75 and -29.40 (m, broad, 7 B). **^{1}H NMR** (δ ppm, DMSO-d6): 0.75 (3H, t, CH_3), 1.10 (2 H, sextuplet, CH_2), 1.25 (4 H, quintuplet, $2CH_2$), 2.15 (2 H, t, CH_2), 7.5-7.8 (20 H, m, H of PPh_4^+).**^{13}C NMR** (DMSO-d6): 166.35, 135.87, 135.10, 131.03, 118.72, 117.69, 32.10, 24.18, 22.72, 14.32. **^{31}P NMR** (DMSO-d6): 22.13. **Mass spectrometry (ESI/MS):** m/z = 216. **Elemental analysis:** % theoretical C: 54.628; H: 6.069. Found C: 52.251; H: 6.906. H/C ratio: 0.13. **Yield:** 80%.

(PPh_4)(MgCl)[2-$B_{10}H_9C(O)C_3H_7$] (**4**) **^{11}B (^{1}H) NMR** (δ ppm, 128 MHz, CD_3CN): 3.30 (d, 2 B), -19.10 (s, 1 B), between -21.94 and -28.42 (m, broad, 7 B). **^{1}H NMR** (δ ppm, DMSO-d6): 0.68 (6 H, d, $2CH_3$), 2.65 (1 H, septuplet, CH), 7.51-8.04 (20 H, m, H of PPh_4^+). ^{13}C NMR (δ ppm, DMSO-d6): 135.75, 135.29, 130.91, 118.71, 117.61, 19.59. **^{31}P NMR** (DMSO-d6): 22.56. **Mass spectrometry (ESI/MS):** m/z = 188. **Elemental analysis:** % theoretical C: 57.250; H: 5.859. Found C: 45.358; H: 5.859. H/C ratio: 0.12. **Yield:** 75%.

(PPh_4)(MgCl) [2-$B_{10}H_9C(O)CH_2CH{=}CH_2$] (**5**) **^{11}B (^{1}H) NMR** (δ ppm, 128 MHz, CD_3CN): 2.56 (d, 1 B), -0.51 (d, 1B) -20.17 (s, 1 B), between -26 and -28 (m, broad, 7 B). **^{1}H NMR** (δ ppm, DMSO-d6): 3.25 (2H, d, CH_2), 4.85 (2H, m, CH2), 5.85 (1H, m, CH), 7.5-7.8 (20H, m, H of PPh_4^+). **^{13}C NMR** (δ ppm, DMSO-d6):164.24, 135.87, 135.09, 134.92, 131.03, 130.84, 118.61, 117.69, 45.95. **^{31}P NMR** (DMSO-d6): 21.64. **Mass spectrometry (ESI/MS):** m/z = 185.20. **Elemental analysis:** % theoretical C: 57.450; H: 5.850. Found C: 57.354; H: 6.521. H/C ratio: 0.10. **Yield:** 68%.

(PPh_4)(MgBr) [2-$B_{10}H_9C(O)CH{=}CH_2$] (**6**) **^{11}B (^{1}H) NMR** (δ ppm, 128 MHz, CD_3CN): 3.78 (d, 1 B), 0.83 (d,1B), -18.62 (s, 1 B), between -25.54 and -31.32 (m, broad, 7 B). **^{1}H NMR** (δ ppm, DMSO-d6): 4.95 (1H, m, CH_2), 5.85 (1 H, m, CH_2),6.49 (1 H, m, CH), 7.5-7.8 (20 H, m H of PPh_4^+).**^{13}C NMR** (δ ppm, DMSO-d6): 175.56, 135.95, 135.10, 134.90, 130.91, 118.72, 117.37. **^{31}P NMR** (DMSO-d6): 22.14. **Mass spectrometry (ESI/MS):** m/z = 171.18. **Elemental analysis:** % theoretical C:52.682; H: 5.203. Found C: 52.456; H: 6.025. H/C ratio: 0.10. **Yield:** 73%.

(PPh_4)(MgBr) [2-$B_{10}H_9C(O)C{\equiv}CCH_3$] (**7**) **^{11}B (^{1}H) NMR** (δ ppm, 128 MHz, CD_3CN): 3.05 (d, 1 B), -0.64 (d, 1B), -18.22 (s, 1 B), between -25.28 and -29.06 (m, broad, 7 B). **^{1}H NMR** (δ ppm, DMSO-d6): 1.75 (3 H, s, CH_3), 7.5-7.8 (20 H, m H of PPh_4^+). **^{13}C NMR** (δ ppm, DMSO-d6): 171.20, 135.95, 134.60, 131.27, 118.61, 117.65, 82.50, 67.50, 3.91. **^{31}P NMR** (DMSO-d6): 22.13. **Mass spectrometry (ESI/MS):** m/z = 184. **Elemental analysis:** % theoretical C: 53.570; H: 5.140. Found C: 52.670; H: 4.912. H/C ratio: 0.09. **Yield:** 70%.

4. Conclusions

In the present work, a selective synthetic approach to produce closo-decaborate derivatives with building block properties was developed. The approach centers on the reaction of the carbonyl derivative [2-$B_{10}H_9CO]^-$ with a Grignard reagent of different constituents. The key derivatives [2-$B_{10}H_9C(O)CH{=}CH_2]^{2-}$, [2-$B_{10}H_9C(O)CH_2CH{=}CH_2]^{2-}$, and [2-$B_{10}H_9C(O)C{\equiv}CCH_3]^{2-}$ comprise the allyl, vinyl and propynyl functionalities which allow the conjugation/polymerization of the closo-decaborate cluster into biological and functional materials.

Author Contributions: Synthesis and solution studies, N.M.; supervision of NMR studies, K.P.; supervision of the work and funding acquisition, A.M. and D.N. All authors have read and agreed to the published version of the manuscript.

Funding: This research was funded by Agence universitaire de la francophonie (AUF), centre national de la recherche scientifique Liban (CNRSL) and Lebanese university (LU). N.M. thanks AUF-CNRSL-UL for financial support.

Institutional Review Board Statement: Not applicable.

Informed Consent Statement: Not applicable.

References

1. Mingos, D.M.P., *50th Anniversary of Electron Counting Paradigms for Polyhedral Molecules: Historical and Recent Developments*. 2022: Springer International Publishing.
2. Moury, R., et al., *Study of the Temperature- and Pressure-Dependent Structural Properties of Alkali Hydrido-closo-borate Compounds.* Inorganic Chemistry, 2022. **61**(13): p. 5224-5233.
3. Zhao, X., et al., *Progress in three-dimensional aromatic-like closo-dodecaborate.* Coordination Chemistry Reviews, 2021. **444**: p. 214042.
4. Klyukin, I.N., et al. *Theoretical Study of closo-Borate Anions [BnHn]2− (n = 5–12): Bonding, Atomic Charges, and Reactivity Analysis*. Symmetry, 2021. **13**, DOI: 10.3390/sym13030464.
5. Voinova, V.V., et al., *Electrochemical Properties of the closo-Decaborate Anion $[B_{10}H_{10}]^{2-}$ and a New Method for Preparation of the [B20H18]2− Anion*. Russian Journal of Inorganic Chemistry, 2021. **66**(3): p. 295-304.
6. Green, M., et al., *Closo-Borate Gel Polymer Electrolyte with Remarkable Electrochemical Stability and a Wide Operating Temperature Window.* Advanced Science, 2022. **9**(16): p. 2106032.
7. Ali, F., N. S Hosmane, and Y. Zhu, *Boron Chemistry for Medical Applications.* Molecules (Basel, Switzerland), 2020. **25**(4): p. 828.
8. Hu, K., et al., *Boron agents for neutron capture therapy.* Coordination Chemistry Reviews, 2020. **405**: p. 213139.
9. Avdeeva, V.V., E.A. Malinina, and N.T. Kuznetsov, *Boron cluster anions and their derivatives in complexation reactions.* Coordination Chemistry Reviews, 2022. **469**: p. 214636.
10. Hosmane, N.S. and R.D. Eagling, *Handbook Of Boron Science: With Applications In Organometallics, Catalysis, Materials And Medicine (In 4 Volumes)*. 2018: World Scientific Publishing Company.
11. Abi-Ghaida, F., A. Mehdi, and D. Naoufal, *Boratosilane Precursors: Integration Into Hybrid Materials*, in *Handbook of Boron Science*. 2018, WORLD SCIENTIFIC (EUROPE). p. 227-250.
12. Diab, M., et al. *Grafting of Anionic Decahydro-Closo-Decaborate Clusters on Keggin and Dawson-Type Polyoxometalates: Syntheses, Studies in Solution, DFT Calculations and Electrochemical Properties*. Molecules, 2022. **27**, DOI: 10.3390/molecules27227663.
13. Diab, M., et al., *Unprecedented coupling reaction between two anionic species of a closo-decahydrodecaborate cluster and an Anderson-type polyoxometalate.* Dalton Transactions, 2020. **49**(15): p. 4685-4689.
14. Payandeh, S., et al., *Nido-Borate/Closo-Borate Mixed-Anion Electrolytes for All-Solid-State Batteries.* Chemistry of Materials, 2020. **32**(3): p. 1101-1110.
15. Duchêne, L., et al., *Crystallization of closo-borate electrolytes from solution enabling infiltration into slurry-casted porous electrodes for all-solid-state batteries.* Energy Storage Materials, 2020. **26**: p. 543-549.

16. Dobbins, T.A., *Overview of the Structure-Dynamics-Function Relationships in Borohydrides for Use as Solid-State Electrolytes in Battery Applications.* Molecules, 2021. **26**(11).
17. Golub, I.E., et al. *Thermodynamic Hydricity of Small Borane Clusters and Polyhedral closo-Boranes*. Molecules, 2020. **25**, DOI: 10.3390/molecules25122920.
18. Huang, Z., et al., *Boron: Its Role in Energy-Related Processes and Applications.* Angewandte Chemie International Edition, 2020. **59**(23): p. 8800-8816.
19. Avdeeva, V.V., et al., *Physiologically Active Compounds Based on Membranotropic Cage Carriers–Derivatives of Adamantane and Polyhedral Boron Clusters (Review).* Russian Journal of Inorganic Chemistry, 2022. **67**(1): p. 28-47.
20. Stogniy, M.Y., et al., *Nitrilium derivatives of polyhedral boron compounds (boranes, carboranes, metallocarboranes): Synthesis and reactivity.* Phosphorus, Sulfur, and Silicon and the Related Elements, 2019. **194**(10): p. 983-988.
21. Sedlák, D., et al., *Structure–Activity Relationship of para-Carborane Selective Estrogen Receptor β Agonists.* Journal of Medicinal Chemistry, 2021. **64**(13): p. 9330-9353.
22. Jin, W.H., et al., *A Review of Boron Neutron Capture Therapy: Its History and Current Challenges.* Int J Part Ther, 2022. **9**(1): p. 71-82.
23. Yorov, K.E., et al., *$[B_{10}H_{10}]^{2-}$ Nanoclusters Covalently Immobilized to Hybrid SiO_2 Aerogels for Slow Neutron Shielding Applications.* ACS Applied Nano Materials, 2022. **5**(8): p. 11529-11538.
24. Abi-Ghaida, F., et al., *New triethoxysilylated 10-vertex closo-decaborate clusters. Synthesis and controlled immobilization into mesoporous silica.* Dalton Transactions, 2014. **43**(34): p. 13087-13095.
25. Abi-Ghaida, F., et al., *Multifunctional Silica Nanoparticles Modified via Silylated-Decaborate Precursors.* Journal of Nanomaterials, 2015. **2015**: p. 608432.
26. Stepanova, M., et al. *Design, Fabrication and Characterization of Biodegradable Composites Containing Closo-Borates as Potential Materials for Boron Neutron Capture Therapy*. Polymers, 2022. **14**, DOI: 10.3390/polym14183864.
27. Mahfouz, N., et al., *Recent Achievements on Functionalization within closo-Decahydrodecaborate $[B_{10}H_{10}]^{2-}$ Clusters.* ChemistrySelect, 2022. **7**(21): p. e202200770.
28. Avdeeva, V.V., et al., *Complexation and exopolyhedral substitution of the terminal hydrogen atoms in the decahydro-closo-decaborate anion in the presence of cobalt(II).* Polyhedron, 2019. **162**: p. 65-70.
29. Kubasov, A.S., et al., *Methods of Creating closo-Decaborate Anion Derivatives with Bridging and Terminal Exopolyhedral Cyclic Substituents of Sulfonium Type.* Doklady Chemistry, 2018. **483**(1): p. 263-265.
30. Zhizhin, K.Y., A.P. Zhdanov, and N.T. Kuznetsov, *Derivatives of closo-decaborate anion $[B_{10}H_{10}]^{2-}$ with exo-polyhedral substituents.* Russian Journal of Inorganic Chemistry, 2010. **55**(14): p. 2089-2127.
31. Sivaev, I.B., A.V. Prikaznov, and D. Naoufal, *Fifty years of the closo -decaborate anion chemistry.* Collection of Czechoslovak Chemical Communications, 2010. **75**: p. 1149-1199.
32. Grimes, R.N., *Carboranes*. 2016: Academic Press.
33. Marfavi, A., P. Kavianpour, and L.M. Rendina, *Carboranes in drug discovery, chemical biology and molecular imaging.* Nature Reviews Chemistry, 2022. **6**(7): p. 486-504.
34. Flieger, S., et al. *Carborane-Containing Hydroxamate MMP Ligands for the Treatment of Tumors Using Boron Neutron Capture Therapy (BNCT): Efficacy without Tumor Cell Entry*. International Journal of Molecular Sciences, 2023. **24**, DOI: 10.3390/ijms24086973.
35. Issa, F., M. Kassiou, and L.M. Rendina, *Boron in Drug Discovery: Carboranes as Unique Pharmacophores in Biologically Active Compounds.* Chemical Reviews, 2011. **111**(9): p. 5701-5722.
36. Ren, H., et al., *Direct B–H Functionalization of Icosahedral Carboranes via Hydrogen Atom Transfer.* Journal of the American Chemical Society, 2023. **145**(13): p. 7638-7647.
37. Dziedzic, R.M. and A.M. Spokoyny, *Metal-catalyzed cross-coupling chemistry with polyhedral boranes.* Chem Commun (Camb), 2019. **55**(4): p. 430-442.
38. Liu, F., et al., *Sonogashira coupling of the ethynyl monocarborane $[CB_{11}H_{11}$-12-$CCH]^{1-}$.* Dalton Transactions, 2022. **51**(29): p. 10880-10886.
39. Eriksson, L., et al., *Palladium-Catalyzed Heck Reactions of Styrene Derivatives and 2-Iodo-p-carborane.* The Journal of Organic Chemistry, 2003. **68**(9): p. 3569-3573.
40. Lennox, A.J.J. and G.C. Lloyd-Jones, *Transmetalation in the Suzuki–Miyaura Coupling: The Fork in the Trail.* Angewandte Chemie International Edition, 2013. **52**(29): p. 7362-7370.
41. Zheng, Z., et al., *Facile Electrophilic Iodination of Icosahedral Carboranes. Synthesis of Carborane Derivatives with Boron-Carbon Bonds via the Palladium-Catalyzed Reaction of Diiodocarboranes with Grignard Reagents.* Inorganic Chemistry, 1995. **34**(8): p. 2095-2100.
42. Tang, C., J. Zhang, and Z. Xie, *Direct Nucleophilic Substitution Reaction of Cage B–H Bonds by Grignard Reagents: A Route to Regioselective B4-Alkylation of o-Carboranes.* Angewandte Chemie International Edition, 2017. **56**(30): p. 8642-8646.
43. El Anwar, S., et al., *Synthesis and characterization of click-decahydrodecaborate derivatives by the copper(I) catalyzed [3+2] azide-alkyne cycloaddition reaction.* Journal of Organometallic Chemistry, 2018. **865**: p. 89-94.

44. Laila, Z., et al., *Clean-activation of the B–H bond in closo-decahydrodecaborate $[B_{10}H_{10}]^{2-}$ anion via soft-route.* Journal of Organometallic Chemistry, 2020. **910**: p. 121132.
45. Laila, Z., et al., *Study of the controlled temperature reaction between closo-decahydrodecaborate and alcohols in H_2SO_4 medium.* Main Group Chemistry, 2015. **14**: p. 301-312.
46. Shelly, K., C.B. Knobler, and M.F. Hawthorne, *Synthesis of monosubstituted derivatives of closo-decahydrodecaborate (2-). X-ray crystal structures of [closo-2-$B_{10}H_9CO]^-$ and [closo-2-$B_{10}H_9NCO]^{2-}$.* Inorganic Chemistry, 1992. **31**(13): p. 2889-2892.
47. Rzeszotarska, E., I. Novozhilova, and P. Kaszyński, *Convenient Synthesis of [closo-B10H9-1-I]2– and [closo-$B_{10}H_8$-1,10-$I_2]^{2-}$ Anions.* Inorganic Chemistry, 2017. **56**(22): p. 14351-14356.
48. Klyukin, I.N., et al., *Study of Protonation of the Monocarbonyl Derivative of the closo-Decaborate Anion $[B_{10}H_9CO]^-$.* Russian Journal of Inorganic Chemistry, 2021. **66**(12): p. 1798-1801.
49. Klyukin, I.N., et al., *Synthesis and Physicochemical Properties of C-Borylated Amides Based on the closo-Decaborate Anion.* Russian Journal of Inorganic Chemistry, 2019. **64**(11): p. 1405-1409.
50. Fink, K. and M. Uchman, *Boron cluster compounds as new chemical leads for antimicrobial therapy.* Coordination Chemistry Reviews, 2021. **431**: p. 213684.
51. Li, J., et al., *Boron encapsulated in a liposome can be used for combinational neutron capture therapy.* Nature Communications, 2022. **13**(1): p. 2143.